Received 00th January 20xx,
Accepted 00th January 20xx

DOI: xxxxxx/x0xx00000x

Integration of Organic Electrochemical Transistors and Immuno-Affinity Membranes for Label-Free Detection of Interleukin-6 at the Physiological Concentration Range through Antibody-Antigen Recognition

Denis Gentili,*[a†] Pasquale D'Angelo,[b†] Francesca Militano,[c†] Rosalinda Mazzei,[c] Teresa Poerio,[c] Marco Brucale,[a] Giuseppe Tarabella,[bd] Simone Bonetti,[e] Simone L. Marasso,[bf] Matteo Cocuzza,[bf] Lidietta Giorno,[c] Salvatore Iannotta[b] and Massimiliano Cavallini[a]

In the present study, we demonstrate the label-free and selective detection of Interleukin-6 (IL-6), a key cell-signaling molecule in biology and medicine, by integrating an OECT with an immuno-affinity regenerated cellulose membrane. The membrane is aimed at increasing the local concentration of IL-6 at the sensing electrode and, thereby, at enhancing the device response for concentrations falling within the physiological concentration range of cytokines. The OECT gate electrode is functionalized with oligo(ethylene glycol)-terminated self-assembled alkanethiolate monolayer (SAM) for both the immobilization of anti IL-6 antibodies and the inhibition of non-specific biomolecule binding. The OECT gate/electrolyte interface is exploited for selective detection of IL-6 through the monitoring of antigen-antibody binding events occurring at the gate electrode.

Introduction

Cytokines are small soluble proteins (~6-70 kDa) secreted by immune and non-immune cells that act as indicators of the functional status of the body and are strongly associated with inflammation or disease progression. Due to this, they are widely used as biomarkers to characterize the immune function, understand and predict disease, and monitor treatment effects. In particular, Interleukin 6 (IL-6) is a pleiotropic cytokine that plays both pro-inflammatory and anti-inflammatory functions that affect processes ranging from immunity to tissue repair and metabolism. IL-6 is produced by T cells, monocytes, fibroblasts, endothelial cells and keratinocytes, and promotes differentiation of B cells, activates cytotoxic T cells, and regulates bone metabolism.[1, 2] Detecting cytokines in solution and measuring their concentration is however a challenging task, since their concentration in body fluids is normally in the pg/mL range. Currently, the most common technique for cytokine detection is the enzyme-linked immunosorbent assay (ELISA), which is a highly sensitive and accurate technique, but suffers from drawbacks such as the relatively large sample volume and long incubation time required, as well as the complicated sample labeling process; all these factors concur to prevent its application to the real-time or dynamic monitoring of cytokines.[2] Conversely, label-free approaches allow minimizing costs, processing time and non-specific binding issues linked to the sample labeling process in complex matrix samples such as blood. Therefore, label-free methods for the direct detection of the antibody-antigen (Ab-Ag) recognition events are currently needed to develop sensitive, selective, and rapid real-time cytokine analysis platforms.

Organic electrochemical transistors (OECTs) are attracting a great deal of attention for applications in medical diagnostics and bioelectronic implants due to their tissue compatibility and the relative ease with which they can be interfaced with biological systems.[3, 4] The OECT architecture enables stable performance in aqueous environment and can be efficiently operated in electrolytes at low voltages (<1 V); due to this, it is an optimally suited platform for developing label-free chemical and biological sensors based on electrical signal transduction, bypassing the need for fluorescent, radio, or enzymatic labels.[5] OECT-based label-free sensors detect recognition events by measuring changes occurring upon interaction with target analytes in the potential drop across the device interfaces. OECTs have been successfully employed as transducers for converting molecular recognition events into physically detectable signals and to develop various chemical sensors (pH,

[a.] *Istituto per lo Studio dei Materiali Nanostrutturati, Consiglio Nazionale delle Ricerche (CNR-ISMN), Via Gobetti 101, 40129 Bologna, Italy. E-mail: denis.gentili@ismn.cnr.it*
[b.] *Istituto dei Materiali per l'Elettronica ed il Magnetismo, Consiglio Nazionale delle Ricerche (CNR-IMEM), Parco Area delle Scienze 37/A, 43124 Parma, Italy.*
[c.] *Istituto per la Tecnologia delle Membrane, Consiglio Nazionale delle Ricerche (CNR-ITM) via Pietro Bucci 17/C, 87036 Rende, Italy.*
[d.] *Camlin Italy Srl, Strada Budellungo 2, 43123 Parma, Italy.*
[e.] *CellDynamics iSRL, via P. Gobetti 101, 40129 Bologna, Italy.*
[f.] *Chilab - Materials and Microsystems Laboratory, Dipartimento di Scienza Applicata e Tecnologia (DISAT), Politecnico di Torino, via Lungo Piazza d'Armi 6, 10034 Chivasso, Italy.*
† These authors contributed equally to this work
Electronic Supplementary Information (ESI) available: Randles equivalent circuit, static water contact angle and AFM images. See DOI: xxxxxxx/x0xx00000x

ions and humidity) and biosensors (glucose, DNA, dopamine and enzyme).[6-9] Despite this, the investigation of immunosensors relying on OECT-based transduction to detect specific antibody-antigen (Ab-Ag) interaction has been sparse, and limited to the electrolyte/channel interface,[10, 11] and there are few examples of label-free immunosensors based on electrochemical transduction for the detection of cytokine in literature, and, to the best of our knowledge, none of these devices is based on an OECT architecture.[2, 12, 13]

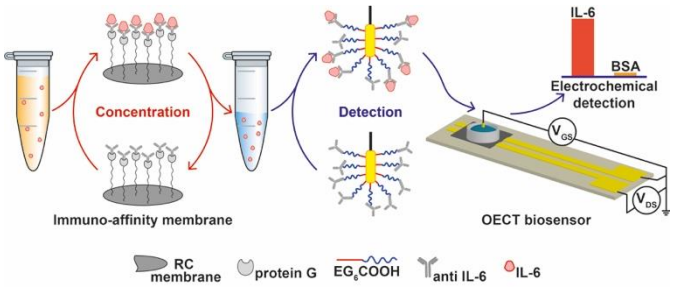

Fig. 1. Schematic illustration of the selective concentration and electrochemical detection of IL-6

In the present work, we demonstrate that the combination of selective capturing membranes and organic-based biosensors represents an efficient strategy for improving the intrinsic device detection capability. Specifically, here we show the label-free detection of cytokine IL-6, for concentrations down to their physiological range, through the integration of an OECT biosensor with an immuno-affinity regenerated cellulose (RC) membrane. The capturing membrane promotes the IL-6 fine detection, as the amount of IL-6 captured by the membrane increases the IL-6 concentration by one order of magnitude, thus favoring the detection for concentrations below the intrinsic detection limit of the device (Fig. 1). We have exploited the gate/electrolyte interface for selectively detect IL-6 via the immobilization of anti IL-6 antibodies, as the recognition reagent, onto the surface of the gate electrode, then monitoring Ab-Ag binding events occurring at the functionalized electrode. We also show that the use of oligo(ethylene glycol) (OEG)-terminated self-assembled alkanethiolate monolayers (SAMs) for the immobilization of antibodies prevents non-specific protein binding, which is one of the major limitations in cytokine analysis,[2] and allows us to selectively detect IL-6.

Results and discussion

Gold (Au) wires, 1 mm in diameter, were used as gate electrodes. The functionalization of the gold (Au) gate electrodes with the recognition species, i.e. anti IL-6, was achieved through chemical immobilization on reactive (i.e. carboxylic acid-terminated) SAMs (Fig. 2a).[14, 15] During the first step of functionalization, Au wire were incubated with an acidified ethanol solution of (11-mercaptoundecyl)hexa(ethylene glycol) acetic acid terminated (EG_6COOH, Fig. 2a). An (OEG)-alkanethiol was preferred to an alkanethiol[16] because EG units are known to reduce nonspecific adhesion of biomolecules and thus, widely used to form protein resistant SAMs on gold surfaces[17-22] and for the passivation of gold nanoparticles.[23] Finally, anti IL-6 antibody was immobilized on the gold electrodes by carbodiimide-mediated amide bond formation via activation of carboxylic acid-terminated SAMs with sulfo-N-hydroxysuccimide.

Functionalization of Au electrodes with EG_6COOH and Ab-Ag binding events occurring at the antibody-functionalized Au electrodes were assessed by cyclic voltammetry (CV) and electrochemical impedance spectroscopy (EIS). Fig. 2b shows voltammetric profiles of a ferri/ferrocyanide solution measured before and after functionalization of Au electrode with EG_6COOH. The bare Au electrode exhibits the well-known reversible peak for the ferri/ferrocyanide redox couple with peak potential shift of approximately 0.1 V. After the adsorption of thiol, the electron transfer of the redox couple is completely inhibited, confirming that a continuous SAM has effectively blocked the electrode surface. EIS is a very powerful tool both to assess the functionalization of electrodes and to detect the biorecognition events on surface-modified electrodes.[24, 25] Fig. 2c shows representative Nyquist plots of an Au electrode after each functionalization and incubation step. After functionalization of bare electrode with EG_6COOH, the diameter of the semicircle in the high frequency region of Nyquist trace increased significantly, indicating a drastic increase of impedance. Modeling the Nyquist plots with a Randles circuit (Fig. S1) shows that, following thiol functionalization, the charge transfer resistance (R_{CT}) increases drastically from 0.006 to 1.2 kΩ cm^2, confirming the blocking behaviour of the SAM. The impedance further increases after antibody immobilization, as shown by the increase in diameter of the semicircle at high frequencies in the Nyquist plot, which in turn testifies an increase of R_{CT} (2.2 kΩ cm^2). After incubating the antibody-functionalized Au electrode with IL-6, the Nyquist plot becomes a large semicircle that extends across the entire range of frequencies and R_{CT} increases up to 4.5 kΩ cm^2, showing that our system is suitable for the direct detection of Ab-Ag recognition events.

The same immobilization procedure was concurrently performed on flat gold-coated surfaces in order to easily monitor, at each functionalization step, the surface wettability and morphology by contact angle goniometry and AFM microscopy, respectively. As shown in Fig. 2d and S2, the static water contact angle value of bare Au (84°) drastically decreases to approximately 40° after thiol functionalization, confirming the formation of SAMs terminating in carboxylic-acid groups,[20] while AFM measurements show that surface roughness (Sq) is largely unaffected by this procedure (Fig. 2d and S2). Conversely, the antibody decoration step barely affects the surface wettability, slightly further increasing the hydrophilicity, but it is accompanied by a significantly increase of Sq. On a qualitative basis, the substrates appear in AFM micrographs as to be thoroughly clean and devoid of any surface decoration prior to their functionalization with the antibody, which causes the appearance of a sparse deposit of small objects with apparent heights of 6-10 nm. The final incubation with IL-6 does not induce significant changes on substrates neither in terms of

wettability nor roughness, even though it seems to increase the number of the larger deposited objects.

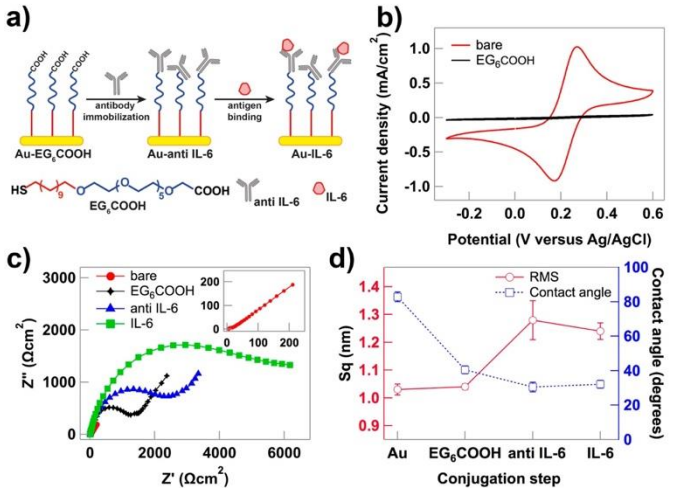

Fig. 2. (a) Schematic illustration of gold electrode functionalization steps. (b) Cyclic voltammograms of bare gold and Au-EG_6COOH electrodes in PBS (pH 7.4) containing 5 mM $[Fe(CN)_6]^{3-/4-}$ redox probe (scan rate: 100 mVs^{-1}). (c) Nyquist plots after each functionalization and incubation step in PBS (pH 7.4) containing 5 mM $[Fe(CN)_6]^{3-/4-}$ redox probe (Frequency measured from 0.05 Hz to 100 kHz with amplitude of 0.1 V and potential applied at +0.22 V). (d) Static water contact angle (blue square) and surface roughness (red circle) values of gold-coated substrates after each functionalization and incubation step.

OECT devices with gate electrodes functionalized with anti IL-6 were used for the immuno-affinity electrochemical detection of IL-6 (Fig. 3a). OECT response to the Ab-Ag recognition was measured in PBS buffer by sweeping V_{GS} between 0 and 0.3 V and fixing V_{DS} at -0.1 V. The sensing capability was assessed by analyzing the current modulation parameter, $\Delta I/I_0$, as a function of gate potential (V_{GS}). $\Delta I/I_0$ has already been proven to be the appropriate figure of merit for OECTs operating in sensing mode, as it provides information about the effective detection of ionic species in solution excluding secondary effects, due to instabilities, that could hinder the sensing response. Current modulation parameters of OECTs working with bare Au-gate electrode or anti IL-6 functionalized Au-gate electrode before and after IL-6 binding were measured in the same operating conditions and are shown in Fig. 3b. The current modulation of OECT was clearly affected by the different nature of the gate electrode, even if the device operation is dominated by the capacitive coupling between device interfaces in contact with the electrolyte [26]. Although Au gate electrodes are expected to promote a less effective ionic diffusion within the PEDOT:PSS film because of a strong V_{GS} drop upon the formation of an electrical double layer (EDL) at the gate/electrolyte interface, [26] our device equipped with a bare Au gate electrode is able to promote a significant current modulation even at low V_{GS} values ($\Delta I/I_0$ ~0.17 at V_{GS} = 0.4 V; see Fig. S4). Following the functionalization of Au gate with anti IL-6 (Fig. 3b, blue curve), $\Delta I/I_0$ undergoes a remarkable decrease. Such decrease can be ascribable to screening effects produced by the immobilized anti IL-6 molecules that, on their turn, modify the capacitive EDL at the gate/electrolyte interface. In fact, a decrease of the EDL capacitance showed by this interface upon antibody immobilization can be related to the increase of the double layer thickness.[27, 28] The EDL capacitance decrease induces a less efficient capacitive coupling between the gate and the channel and a current modulation decrease is expected because of the weakening of the driving force governing the ion drifting towards the active channel.[26, 29] The OECT response upon Ab-Ag interaction (Fig. 3b, orange curve), achieved by incubation of gate electrodes functionalized with anti IL-6 in a reference solution of IL-6 2.2 µg/mL (100 nM), shows an increase of the current modulation with respect to that measured before IL-6 binding, indicating an enhancement of the EDL capacitance. Noteworthy, the extent of current modulation is well above the Limit of Detection (LoD, black dashed line) calculated according to IUPAC recommendation,[16] i.e. using the formula $(\Delta I/I_0)_{mean}+3\sigma$ whereby $(\Delta I/I_0)_{mean}$ is the average response of blank samples and σ_{blank} is the relative standard deviation.

Despite the complex nature of the Ab-Ag interaction, we can argue that upon IL-6 binding a surface dipole that partly compensates the decrease of the interfacial capacitance, due to the screening effect of the antibody, is formed. Gate functionalization of OECT sensors has been demonstrated to produce an analogous effect on current modulation curves, and the shift of such curves has been attributed to an offset voltage that is responsible of the gate voltage drop.[29, 30] Regardless of the origin of changes in EDL capacitance, capacitive immunosensors have demonstrated an increase of the EDL capacitance at the antibody-functionalized interfaces because of the growing number of activated antigen/antibody sites.[31, 32]

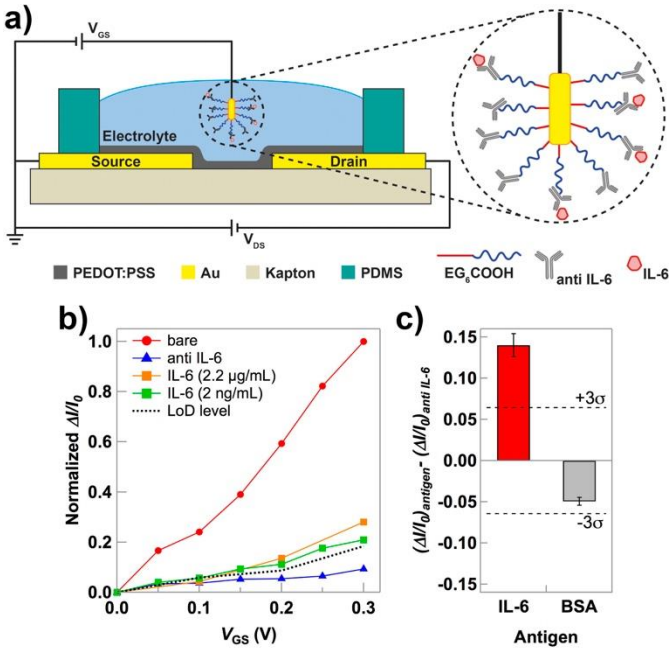

Fig. 3. (a) Cross-sectional representation of the OECT-based immunosensor. (b) Normalized $\Delta I/I_0$ parameter as a function of V_{GS} (V_{DS} at -0.1 V) of OECT working with bare Au gate electrode (red line) and anti IL-6 functionalized Au gate electrode before (blue line) and after incubation in a reference solution of IL-6 2.2 µg/mL (100 nM, green line) and IL-6 2 ng/mL (90 pM, orange line), and LoD level (black dashed line). (c) Change of current modulation of anti IL-6 functionalized Au gate electrode after incubation in a reference solution of IL-6 2.2 µg/mL (100 nM) or BSA 6.6 µg/mL (100 nM) calculated at V_{GS}= 0.3 V as $(\Delta I/I_0)_{antigen} - (\Delta I/I_0)_{anti\ IL\text{-}6}$ (where $(\Delta I/I_0)_{antigen}$ = current modulation of anti IL-6 functionalized Au gate electrode after incubation in a reference solution of IL-6 or BSA

and $(\Delta I/I_0)_{anti\ IL\text{-}6}$ = current modulation of anti IL-6 functionalized Au gate electrode). Dashed lines indicate 3 times the standard deviation of the average response of blank samples.

In contrast to what previously described for IL-6, as shown Fig. 3c, the current modulation of the antibody-functionalized Au electrode was not affected significantly by the incubation in a reference solution containing an equivalent molar concentration of BSA, i.e. 6.6 µg/mL (100 nM), indeed the change of current modulation is less than ±3σ of the current modulation of blank samples This result shows that the use of OEG-terminated SAMs for the immobilization of anti IL-6 allows us to prevent non-specific binding of biomolecules and selectively detect the IL-6.

As shown in Fig. 3b (green curve), a detectable current modulation, i.e. above the LoD level, was successfully measured for antibody-functionalized gate electrodes incubated in reference solutions of IL-6 with a concentration down to 2 ng/mL (90 pM), which is a value at least one order of magnitude higher than the physiologically relevant concentration range of IL-6 (< 0.3 ng/mL[33, 34]). With the aim of exploiting our immuno-electrochemical IL-6 detection system in the physiological range, we implemented an IL-6 pre-concentration system based on an immuno-affinity cellulose membrane whose binding affinity towards IL-6 can be modulated by pH variation, since it is characterized by a high capture ability of IL-6 at pH=7.4 and selective desorption at pH=2.5 (Fig. 4a). The immuno-affinity RC membrane was prepared by functionalization with protein G and subsequent immobilization of anti IL-6 following the procedure reported in ref.[35].

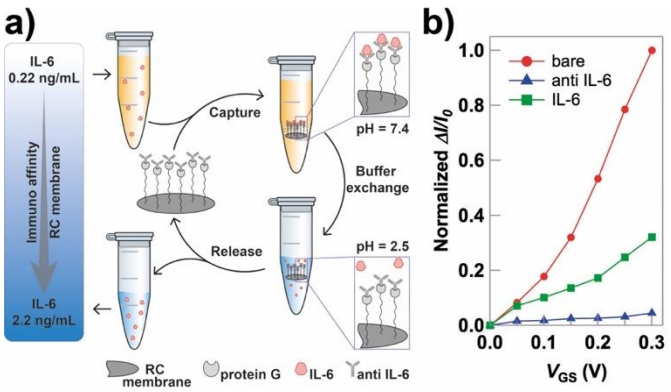

Fig. 4. (a) Schematic representation of the IL-6 pre-concentration by using the immuno-affinity RC membrane. (b) Normalized $\Delta I/I_0$ parameter as a function of V_{GS} of OECT working with bare Au-gate electrode (red curve) and anti IL-6 functionalized Au-gate electrode before (blue curve) and after (green curve) incubation in a pre-concentrated solution of IL-6 0.22 ng/mL (10 pM) upon IL-6 release from the membrane.

As shown schematically in Fig. 4a, the IL-6 concentration increase was obtained by immersing the RC membrane in a 0.22 ng/mL (10 pM) solution in PBS buffer, i.e. with an antigen concentration below the detection limit of our OECTs but within the physiological range of IL-6, and the subsequent desorption in a volume of glycine-HCl buffer to achieve an IL-6 solution with a concentration of 2.2 ng/mL (100 pM), thus above the detection limit. The concentrated solution was subsequently used for the IL-6 electrochemical detection and, as shown in Fig. 4b, the OECT current modulation, measured after the incubation of the anti IL-6 functionalized Au-gate electrode in the pre-concentrated IL-6 solution, shows a trend that is completely in agreement with what was observed above (Fig. 3b, d). These results show that the implementation of a pre-concentration step based on immune-affinity membranes does not affect the electrochemical detection of IL-6, but rather it enables the detection of IL-6 at physiologically relevant concentrations.

Experimental

Materials

1-Ethyl-3-(3-dimethylaminopropyl)carbodiimide hydrochloride (EDC), N-hydroxysulfosuccinimide (sulfo-NHS), dodecyl benzene sulfonic acid (DBSA), sodium periodate ≥ 99.8 %, ethylenediamine, glutaraldehyde, glycine, 2-(N-morpholino)ethanesulfonic acid (MES), and phosphate buffered saline (PBS) were purchased from Sigma-Aldrich and used without further purification. (11-mercaptoundecyl)hexa(ethylene glycol) acetic acid terminated (EG_6COOH) was purchased from ProChimia Surfaces and used without further purification. Sodium borohydride > 98 % was purchased from Thermo Fisher Scientific. PEDOT:PSS (PH 1000) aqueous solution was purchased from Haereous Clevios GmbH and stored at 4 °C. Recombinant protein G (from Streptococcus sp. expressed in E. Coli) and mouse interleukin-6 (IL-6) were purchased from BioVision (Vinci-Biochem). Anti-mouse IL-6 monoclonal antibody (Anti IL-6, 6B4 IGH 54) was purchased from Enzo Life Science (3V Chimica Srl). Flat-sheet regenerated cellulose (RC) membranes (diameter 47 mm) were purchased from Millipore. All aqueous solutions and phosphate-buffered saline (PBS; 10 mM Na_2HPO_4, 1.8 mM KH_2PO_4, 137 mM NaCl, and 2.7 mM KCl, pH 7.4) were prepared with ultrapure water obtained using an ultrafiltration system (Milli-Q, Millipore) and having a measured resistivity of at least 18.2 MΩ·cm.

Gate electrode functionalization

Gold wires (1 mm in diameter) were used as gate electrodes. All electrodes were cleaned with piranha solution (70:30, H_2SO_4:H_2O_2; caution highly oxidative solution) for 20 min, rinsed with deionized water, electropolished in H_2SO_4 (1M), and finally rinsed again with deionized water. Gold electrodes were immersed overnight in an acidified (pH~2) ethanol solution of EG_6COOH (0.5 mM) then rinsed with ethanol and sonicated for 2 min in acidified ethanol and for 2 min in deionized water.[36] Conjugation of anti IL-6 was performed by a two-step coupling procedure.[37] In brief, gold electrodes functionalized with EG_6COOH were reacted with EDC (0.4 M) and sulfo-NHS (0.2 M) in MES buffer (100 mM, pH=5.5) for 30 min, washed with PBS, and then incubated with anti IL-6 (0.1 mg/mL) in PBS for 2h and then rinsed with PBS. Finally, after quenching unreacted sulfo-NHS esters with ethanolamine (100 mM) in PBS, gold electrodes were rinsed and stored in PBS at 4°C.

IL-6 capture

The gate electrodes functionalized with anti IL-6 were incubated with 100 µL of IL-6 or BSA solution in PBS for 1 h. Afterwards, the electrodes were rinsed with PBS (pH=7) and used for the electrochemical detection.

Gold film functionalization

Gold-coated substrates were prepared by thermal evaporation of 5 nm titanium adhesion layer and 50 nm thick gold layer onto microscope slides. Before use, the gold-coated substrates were cut into pieces (10×10 mm^2) and cleaned by immersion in H_2SO_4 (1M) for 60 s and then rinsed with deionized water. The gold films were functionalized according to the procedure used for the gate electrodes.

Morphology measurements

AFM images were collected in PBS on a Multimode 8 microscope operated in PeakForce mode and equipped with a fluid cell, a type J scanner (Bruker Nano Inc. GmbH, Berlin, Germany) and SNL-A probes with a nominal spring constant of 0.35 N/m (Bruker AFM Probes, Camarillo, CA). PBS was microfiltered with regenerated cellulose syringe filters (pore size 0.22 µm) immediately prior to use. Background interpolation and surface roughness parameter calculations were performed with Gwyddion 2.48 (http://gwyddion.net/).[38] The morphology was monitored via AFM microscopy performed in PBS and then quantitatively characterized via the root mean square (RMS) surface roughness descriptor Sq. Reported Sq values are the average of at least three different regions, with the standard deviation of these measures as the uncertainty. Since occasionally samples, including untreated substrates, were characterized by the presence of mechanical abrasions (scratches), we filtered them out of the recorded data by applying a simple high-pass height threshold, only considering the top 30 % of recorded Z values (corresponding to unscratched zones) for successive quantitative analysis. The top, flat areas of the untreated samples were found to be sufficiently homogeneous (starting from 1 μm^2 areas upwards) to calculate significant Sq values.

Contact angle measurements

The static water contact angles of the sample surfaces were measured at 25 °C in air using a contact angle meter (GBX Digidrop instrument) on the basis of the sessile drop method.[39] All of the contact angles were determined by averaging measured values of at least three different points on each sample surface and with the standard deviation of these measures as the uncertainty.

Immuno-affinity membrane RC-PG-Ab-(GA) preparation

The immuno-affinity membranes were prepared following the method reported elsewhere.[35, 40] Briefly, RC membranes were cut into discs of 1 cm diameter and reacted with sodium periodate (0.2 % w/w) in water for 7 h. Afterwards, a spacer was introduced by means of a reaction with ethylenediamine (5 % w/w) in water for 15 h and subsequently with glutaraldehyde (5 % w/w) in water for 2 h. The functionalized membrane discs were equilibrated in PBS (pH=7) and incubated with protein G (1 g/L) in PBS (pH=7) for 3 h. Then, RC membranes were incubated with glycine (1M, pH=7) in water for 14 h, quenching the unreacted aldehyde groups, and then with anti IL-6 antibody (0.5 mg/mL) in PBS (pH=5.8) at 4 °C overnight. A final antibody stabilization step was performed by immersing the membranes in glutaraldehyde (2 % v/v) for 2 h.

IL-6 pre-concentration

The RC-PG-Ab-(GA) membrane was incubated with 1 mL of IL-6 solution (0.22 ng/mL) in PBS for 2 h. After IL-6 loading, the RC-PG-Ab-(GA)-IL-6 membrane was recovered and rinsed with PBS (pH=7). Then, IL-6 was released by incubating the membrane in 100 µL of glycine-HCl buffer (pH=2.5) for 30 minutes. The pH of the IL-6 concentrated solution was adjusted to 7 using NaOH (1M) before the electrochemical detection.

Device fabrication

OECTs with a channel length (L) of 100 µm and a channel width (W) of 6 mm were fabricated on 2-inches circular-shaped Kapton (DuPont) substrates. Gold (100 nm)/Titanium (20 nm) electrodes were deposited by using a Kurt J. Lesker PVD 75 DC Magnetron Sputtering and photo-lithographically patterned by a lift-off process (AZ5214E photoresist, Microchemicals GmbH). A 20 nm-thick film PEDOT: PSS was deposited by spin-coating a mixture of PEDOT:PSS, ethylene glycol (20:1 in volume) and DBSA (0.05 %) and subsequently baked at 150 °C in vacuum for 90 min. The as-prepared PEDOT:PSS film was patterned by a wet etching process. In brief, a 150 nm-thick Ag layer was deposited through a shadow mask using an ULVAC EBX-14D electron beam evaporator and the PEDOT:PSS excess was removed by O_2 plasma (100 mTorr, 100 W, 30 s). Finally, the Ag protective layer was removed by wet etching (E6 Metal Etching, 16 V H_3PO_4 (85 %) : 1V HNO_3 (65 %) : 1V CH_3COOH : 2V H_2O).[41]

Electrochemical measurements

Cyclic voltammetry and electrochemical impedance spectroscopy were carried out in a three-electrode cell equipped with a gold wire as working electrode, an Ag/AgCl reference electrode and a large area platinum foil as counter electrode in PBS (pH 7.4) containing 5 mM $[Fe(CN)_6]^{3-/4-}$ and using a µ-Autolab type III (Metrohm Autolab) potentiostat equipped with a frequency response analyzer. All of the given potentials are reported with respect to the Ag/AgCl reference electrode.

Device measurements

OECT electrical response was evaluated using a PBS solution as electrolyte and an Agilent Source Measure Unit B2902A controlled by a customised LabView routine. All electrical measurements were carried out in ambient atmosphere. Label-free detection of IL-6 in PBS solutions was carried out by acquiring channel current vs. time curves (I_{DS} vs. time) at a fixed source-drain voltage (V_{DS} = -0.1 V) and by applying 10 seconds

lasting rectangular-shaped voltage pulses at the gate terminal (V_{GS}), in the voltage range between 0 and 0.3 V (step 0.05 or 0.1 V). Analysis of the OECT response was performed by extracting the current modulation parameter $\Delta I/I_0$ from I_{DS} vs. time curves, defined as $\Delta I/I_0 = [(I - I_0)/I_0]$, where I is the I_{DS} measured for $V_{GS} > 0$ V (off state), and I_0 is the I_{DS} value for $V_{GS} = 0$ V (on state).[42, 43]

Conclusions

In conclusion, we have reported an immunosensor based on an OECT integrated with an immuno-affinity membrane for the label-free and selective detection of IL-6 at physiologically relevant concentrations. The OECT gate/electrolyte interface has been exploited for selectively detect the presence of IL-6 through the monitoring of Ag-Ab binding events occurring at the gate electrode. The functionalization of the gate electrodes with OEG-terminated alkanethiolate SAMs allowed us to immobilize anti IL-6 antibodies while inhibiting non-specific biomolecule binding. The integration of immuno-affinity regenerated cellulose membranes with the sensing OECT allowed us to improve the detection limit down to the pg/mL concentration range. In summary, our results show that the OECT gate/electrolyte interface can be conveniently exploited for the label-free and effective detection of Ag-Ab recognition events, and that the integration of an antigen pre-concentration step with the OECT is a suitable strategy to improve the detection limit by at least one order of magnitude, paving the way to the development of microfluidic integrated label-free OECT-based immunosensors.

Conflicts of interest

There are no conflicts to declare

Acknowledgements

This work was supported by the Italian flagship NANOMAX, N-CHEM.

Notes and references

1. G. Arango Duque and A. Descoteaux, *Front. Immunol.*, 2014, **5**.
2. G. Liu, M. Qi, M. R. Hutchinson, G. Yang and E. M. Goldys, *Biosens. Bioelectron.*, 2016, **79**, 810-821.
3. J. Rivnay, R. M. Owens and G. G. Malliaras, *Chem. Mater.*, 2014, **26**, 679-685.
4. K. Svennersten, K. C. Larsson, M. Berggren and A. Richter-Dahlfors, *Biochim. Biophys. Acta*, 2011, **1810**, 276-285.
5. M. A. Cooper, *Anal. Bioanal. Chem.*, 2003, **377**, 834-842.
6. P. Lin and F. Yan, *Adv. Mater.*, 2012, **24**, 34-51.
7. H. Tang, P. Lin, H. L. W. Chan and F. Yan, *Biosens. Bioelectron.*, 2011, **26**, 4559-4563.
8. C. Liao, C. Mak, M. Zhang, H. L. W. Chan and F. Yan, *Adv. Mater.*, 2015, **27**, 676-681.
9. H. Tang, F. Yan, P. Lin, J. Xu and H. L. W. Chan, *Adv. Funct. Mater.*, 2011, **21**, 2264-2272.
10. M. Kanungo, D. N. Srivastava, A. Kumar and A. Q. Contractor, *Chem. Commun.*, 2002, DOI: 10.1039/B111728A, 680-681.
11. D.-J. Kim, N.-E. Lee, J.-S. Park, I.-J. Park, J.-G. Kim and H. J. Cho, *Biosens. Bioelectron.*, 2010, **25**, 2477-2482.
12. A. Baraket, M. Lee, N. Zine, M. Sigaud, J. Bausells and A. Errachid, *Biosens. Bioelectron.*, 2017, **93**, 170-175.
13. X. Luo and J. J. Davis, *Chem. Soc. Rev.*, 2013, **42**, 5944-5962.
14. C. Nicosia and J. Huskens, *Mater. Horiz.*, 2014, **1**, 32-45.
15. D. Gentili, M. Barbalinardo, I. Manet, M. Durso, M. Brucale, A. Mezzi, M. Melucci and M. Cavallini, *Nanoscale*, 2015, **7**, 7184-7188.
16. E. Macchia, M. Ghittorelli, F. Torricelli and L. Torsi, 2017.
17. S. Herrwerth, W. Eck, S. Reinhardt and M. Grunze, *J. Am. Chem. Soc.*, 2003, **125**, 9359-9366.
18. M. W. A. Skoda, R. M. J. Jacobs, J. Willis and F. Schreiber, *Langmuir*, 2007, **23**, 970-974.
19. L. Y. Li, S. F. Chen, J. Zheng, B. D. Ratner and S. Y. Jiang, *J. Phys. Chem. B*, 2005, **109**, 2934-2941.
20. J. K. Lee, Y. G. Kim, Y. S. Chi, W. S. Yun and I. S. Choi, *J. Phys. Chem. B*, 2004, **108**, 7665-7673.
21. P. Harder, M. Grunze, R. Dahint, G. M. Whitesides and P. E. Laibinis, *J. Phys. Chem. B*, 1998, **102**, 426-436.
22. K. L. Prime and G. M. Whitesides, *Science*, 1991, **252**, 1164-1167.
23. D. Gentili, G. Ori, L. Ortolani, V. Morandi and M. Cavallini, *ChemNanoMat*, 2017, **3**, 874-878.
24. E. Katz and I. Willner, *Electroanalysis*, 2003, **15**, 913-947.
25. E. P. Randviir and C. E. Banks, *Anal. Methods*, 2013, **5**, 1098-1115.
26. G. Tarabella, C. Santato, S. Y. Yang, S. Iannotta, G. G. Malliaras and F. Cicoira, *Appl. Phys. Lett.*, 2010, **97**, 123304.
27. M. Bart, E. C. A. Stigter, H. R. Stapert, G. J. de Jong and W. P. van Bennekom, *Biosens. Bioelectron.*, 2005, **21**, 49-59.
28. A. Gebbert, M. Alvarez-Icaza, W. Stoecklein and R. D. Schmid, *Anal. Chem.*, 1992, **64**, 997-1003.
29. P. Lin, F. Yan and H. L. W. Chan, *ACS Appl. Mater. Interfaces*, 2010, **2**, 1637-1641.
30. P. Lin, X. Luo, I. M. Hsing and F. Yan, *Adv. Mater.*, 2011, **23**, 4035-4040.
31. C. Berggren, B. Bjarnason and G. Johansson, *Biosens. Bioelectron.*, 1998, **13**, 1061-1068.
32. C. Berggren and G. Johansson, *Anal. Chem.*, 1997, **69**, 3651-3657.
33. J. Huang, H. Chen, W. Niu, D. W. H. Fam, A. Palaniappan, M. Larisika, S. H. Faulkner, C. Nowak, M. A. Nimmo, B. Liedberg and A. I. Y. Tok, *RSC Adv.*, 2015, **5**, 39245-39251.
34. F. Riedel, I. Zaiss, D. Herzog, K. Götte, R. Naim and K. Hörmann, *Anticancer Res.*, 2005, **25**, 2761-2765.
35. F. Militano, T. Poerio, R. Mazzei, S. Salerno, L. D. Bartolo and L. Giorno, *Biosens. Bioelectron.*, 2017, **92**, 54-60.
36. I. Zaccari, B. G. Catchpole, S. X. Laurenson, A. G. Davies and C. Wälti, *Langmuir*, 2014, **30**, 1321-1326.
37. G. T. Hermanson, *Bioconjugate Techniques (Third edition)*, Academic Press, Boston, 2013.
38. D. Nečas and P. Klapetek, *Cent. Eur. J. Phys.*, 2012, **10**, 181-188.
39. F. Lugli, G. Fioravanti, D. Pattini, L. Pasquali, M. Montecchi, D. Gentili, M. Murgia, Z. Hemmatian, M. Cavallini and F. Zerbetto, *Adv. Funct. Mater.*, 2013, **23**, 5543–5549.

40. F. Militano, T. Poerio, R. Mazzei, E. Piacentini, A. Gugliuzza and L. Giorno, *Colloids Surf. B*, 2016, **143**, 309-317.
41. S. Ouyang, Y. Xie, D. Zhu, X. Xu, D. Wang, T. Tan and H. H. Fong, *Org. Electron.*, 2014, **15**, 1822-1827.
42. D. A. Bernards, D. J. Macaya, M. Nikolou, J. A. DeFranco, S. Takamatsu and G. G. Malliaras, *J. Mater. Chem.*, 2008, **18**, 116-120.
43. F. Cicoira, M. Sessolo, O. Yaghmazadeh, J. A. DeFranco, S. Y. Yang and G. G. Malliaras, *Adv. Mater.*, 2010, **22**, 1012-1016.